Nuclear Engineering and Technology 51 (2019) 1957–1963

Contents lists available at ScienceDirect

Nuclear Engineering and Technology

journal homepage: www.elsevier.com/locate/net

Original Article

Studies on decomposition behavior of oxalic acid waste by UVC photo-Fenton advanced oxidation process

Jin-Hee Kim [a], Hyun-Kyu Lee [b], Yoon-Ji Park [a], Sae-Binna Lee [a], Sang-June Choi [a, b], Wonzin Oh [b, *], Hak-Soo Kim [c], Cho-Rong Kim [c], Ki-Chul Kim [d], Bum-Chul Seo [d]

[a] School of Architectural, Civil, Environmental, and Energy Engineering, Kyungpook National University, 80 Daehak-ro, Buk-gu, Daegu, 41566, Republic of Korea
[b] Research Institute of Advanced Energy Technology, Kyungpook National University, 80 Daehak-ro, Buk-gu, Daegu, 41566, Republic of Korea
[c] KHNP Central Research Institute, 70, Yuseong-daero 1312beon-gil, Yuseong-gu, Daejeon, Republic of Korea
[d] KEPCO KPS, 96-1 Gilchon-Gil, Jangan-Eup, Gijang-Gun, Busan, Republic of Korea

ARTICLE INFO

Article history:
Received 15 November 2018
Received in revised form
24 May 2019
Accepted 8 June 2019
Available online 12 June 2019

Keywords:
AOP
UVC photo-Fenton
Chemical decontamination waste
Oxalic acid

ABSTRACT

A UVC photo-Fenton advanced oxidation process (AOP) was studied to develop a process for the decomposition of oxalic acid waste generated in the chemical decontamination of nuclear power plants. The oxalate decomposition behavior was investigated by using a UVC photo-Fenton reactor system with a recirculation tank. The effects of the three operational variables—UVC irradiation, H_2O_2 and Fenton reagent—on the oxalate decomposition behavior were experimentally studied, and the behavior of the decomposition product, CO_2, was observed. UVC irradiation of oxalate resulted in vigorous CO_2 bubbling, and the irradiation dose was thought to be a rate-determining variable. Based on the above results, the oxalate decomposition kinetics were investigated from the viewpoint of radical formation, propagation, and termination reactions. The proposed UVC irradiation density model, expressed by the first-order reaction of oxalate with the same amount of H_2O_2 consumption, satisfactorily predicted the oxalate decomposition behavior, irrespective of the circulate rate in the reactor system within the experimental range.

1. Introduction

Advanced oxidation processes (AOPs) based on the UV-photo Fenton reaction are commonly used for decomposition of low concentration organic waste, less than several ppm. Typical example is to decompose persistent trace organic contaminants as part of wastewater treatment processes aimed at reusing water or discharging it to the environment [1–5]. However, there are very few studies on high concentrations of organic waste of several thousand ppm. Past studies on UV photo-Fenton AOPs have focused on the kinetics of hydroxyl radical production and termination, as well as the reaction of the low concentration target organics with hydroxyl radicals [6–8].

Previous comparative study on the decomposition of oxalic acid (Ox) at relatively high concentrations (0.032 mol/L = 2880 ppm) by using UV/H_2O_2/TiO_2, UV/H_2O_2/Fe, and UV/H_2O_2/Fe/TiO_2 systems has focused on the effect of the process variables, i.e., H_2O_2: Ox: Fe molar ratio and TiO_2 addition [9]. 15 W UVA irradiation with a wavelength of 350–410 nm was used.

In addition, the study paid little attention to the most important variable, the UV irradiation dose. They concluded that 1) H_2O_2, Fe, and TiO_2 are the important variables for the UVA-AOP; 2) H_2O_2 is the most important oxidant; and 3) the UVA/H_2O_2/Fe AOP involves homogeneous photolysis and is better than the UVA/H_2O_2/TiO_2 AOP.

In general, as shown in Fig. 2, UVA energy (350–410 nm) penetrates well in oxalic acid solution of several thousand ppm, but the UVC energy (254 nm) used in this study can hardly penetrate the oxalic acid solution and the UVC energy is mostly absorbed in the oxalic acid solution near the lamp surface.

Oxalic acid is widely used as an organic reducing agent for chemical decontamination because it has very high acidity ($pK_{a1} = 1.2$) and is easily decomposed to CO_2. Oxalic acid wastes are generated in large quantities of around several hundred tons from the chemical decontamination of nuclear power plants (NPP) [10].

* Corresponding author.
E-mail address: wonzin@knu.ac.kr (W. Oh).

https://doi.org/10.1016/j.net.2019.06.011

In this study, we investigated the decomposition behavior of concentrated oxalic acid waste including ferrous ions that was generated from the chemical decontamination of an NPP. The important differences between our study and the previous study [9] are the use of UVC energy (254 nm) and consideration of the effect of UVC energy irradiation on the oxalate decomposition behavior. The UVC energy (254 nm) generated by a low-pressure amalgam lamp is absorbed almost 100% in the concentrated oxalate medium and it influences in the radical generation reaction with H_2O_2 and Fenton reagent.

The classical Fenton mechanism [11–14] is shown below, which involves slow radical regeneration reaction of Fenton reagent, Fe^{2+} in equation (2):

$$Fe^{2+} + H_2O_2 + H^+ \rightarrow Fe^{3+} + \cdot OH + H_2O \quad (1)$$

$$Fe^{3+} + H_2O_2 \rightarrow Fe^{2+} + \cdot O_2H + H^+ \quad (2)$$

$$RH + \cdot OH \rightarrow R\cdot + H_2O \quad (3)$$

A UV photo-Fenton AOP was developed with the aim of accelerating ·OH production in the classical Fenton process by using the high UV oxidation potential. The important radical formation steps including radical termination in the UV photo-Fenton AOP were known as follows [15]:

$$H_2O_2 + hv \rightarrow 2 \cdot OH \quad (4)$$

$$Fe^{3+} + H_2O + hv \rightarrow Fe^{2+} + \cdot OH + H^+ \quad (5)$$

$$Fe(OH)^{2+} + H_2O + hv \rightarrow Fe^{2+} + \cdot OH + H^+ \quad (6)$$

$$OH + \cdot OH \rightarrow H_2O_2 \quad (7)$$

$$Fe^{3+} + \cdot OH + H^+ \rightarrow Fe^{2+} + H_2O \quad (8)$$

The radical propagation reaction proceeds until it meets termination reactions, so that scavenger chemicals are often used to prevent them.

The ferric ions are known to be reconverted into Fe^{2+} as in equation (5) at pH < 2 and in equation (6) at pH > 3 [16]. In particular, in the oxalic acid medium, the ferric ions are in the form of the ferric anions $Fe(C_2O_4)_2^-$, which are very stable and difficult to decompose, while the ferrous ions above a certain concentration are precipitated in the form of FeC_2O_4 [17].

Unlike the low concentration organic waste decomposition, in the case of high concentration organic waste decomposition of several thousand ppm, the acidity change greatly depending on the organic decomposition reaction. For example, when the concentration of oxalic acid changes from 3000 ppm to 3 ppm by decomposition, the pH rises from 1.6 to 4.5 by dissociation of oxalic acid. In this study, acidity and temperature were determined by oxalic acid decomposition without external control.

Therefore, the following process parameters are mainly considered for developing a UVC photo-Fenton AOP for oxalic acid decomposition and to find the rate-determining variables in the oxalic acid decomposition system:

1) UVC irradiation dose, H_2O_2 concentration, and Fe^{2+} concentration to distinguish their order of influence
2) Optimum H_2O_2 concentration depending on the initial oxalate concentration
3) Oxalic acid decomposition kinetics
4) Recirculation flow rate and the degree of turbulence in the UVC reactor, including the agitation by CO_2 generation
5) UVC irradiation dose depending on the oxalic acid concentration and volume, and its penetration depth depending on the concentrations of oxalic acid and H_2O_2.

2. Materials and methods

2.1. Chemicals

In this study, ferrous chloride, oxalic acid, and H_2O_2 were used in the photo-Fenton treatment of oxalic acid. All the chemicals were of analytical grade and used without further purification. Iron (II) chloride tetrahydrate ($FeCl_2 \cdot 4H_2O$, extra-pure grade), oxalic acid dehydrate ($H_2C_2O_4 \cdot 2H_2O$, extra-pure grade) and hydrogen peroxide (H_2O_2, ≥28.0%) were obtained from Duksan Chemical Co. (Republic of Korea). Deionized (DI) water was used to prepare simulated oxalic acid waste.

2.2. Photoreactor and UV light source

A schematic of the cylindrical apparatus is shown in Fig. 1. The reactor was made of polished SUS material, and continuous circulation of the solution was achieved by means of a peristaltic pump. A 120 W amalgam lamp, which emits 254 nm light, was set at the center of the reactor. The solution was sampled through a valve installed at the bottom of the reactor for total organic carbon (TOC) measurements.

2.3. Methods

Simulated organic waste of the desired concentration in each experiment was placed in the photoreactor. The oxalic acid waste was appropriately circulated using the peristaltic pump, and decomposition was initiated by operating the UV lamp. The volume of the organic waste to be filled in the reactor (V_R) was set at 3 L. To vary the overall waste volume ($V_W = V_R + V_T$), the mixing tank was connected to the reactor, as shown in Fig. 1. In the mixing tank, the stirring was maintained at 300 rpm using the agitator. For TOC measurements, 10 mL of the sample was withdrawn from the reactor at predetermined time intervals. In the preliminary experiments, increase in temperature up to 95 °C showed no decomposition performance improvement, so that temperature variation

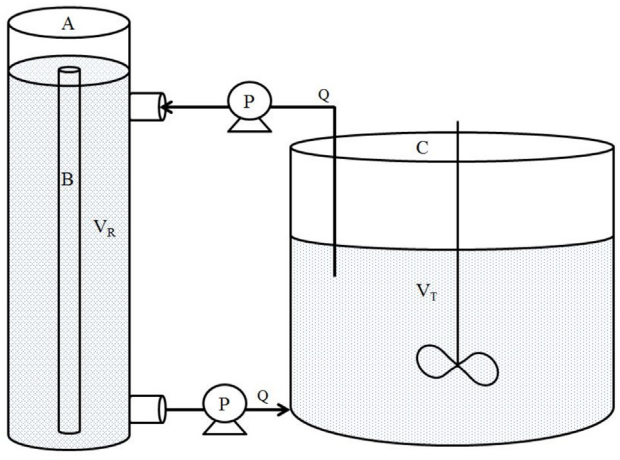

Fig. 1. Schematic of photoreactor used for photo-Fenton treatment.

was not considered in the study. All experiments were carried out at room temperature without external cooling or heating control.

To investigate the decomposition behavior of oxalic acid by photo-Fenton treatment, TOC was measured using a TOC analyzer (TOC-V CPH, SHIMADZU, Japan).

3. Results and discussion

3.1. Brief comparison of photo-Fenton variables to evaluate rate-determining effect

A low-pressure UVC lamp is often used in UVC photo-Fenton AOPs, and it provides UVC radiation with a typical wavelength of 254 nm. However, UVC is strongly absorbed by organic media, and hence, it cannot penetrate a highly concentrated organic medium. UV transmittance is important factor in designing the UV reactor and the UVC energy transmittance depending on the depth of the medium can be expressed by Beer–Lambert's law in the case of a uniform attenuation medium:

$$T(x) = \exp\left(-\frac{0.693x}{L_h}\right), \quad where\ L_h = \frac{-0.693}{\ln(T_{x=1cm})} \tag{9}$$

where T(x) is a transmission fraction at the distance, x [cm] from the surface of the lamp; L_h is a half transmission length at which the transmission percentage is 50%. As an example, the transmission percentage, T (x = 1 cm), of 254 nm UVC radiation is about 2.9% in 30 mmol/L oxalate medium and 11.5% in 30 mmol/L H_2O_2 medium, as shown in Fig. 2. Thus, the half-transmittance distance from the lamp surface, (L_h) in the 30 mmol/L oxalic acid and H_2O_2 medium are 0.196 cm and 0.32 cm, respectively. This indicates that the UVC irradiation of 30 mmol/L oxalic acid at a distance of 1 cm ($\fallingdotseq 5\ L_h$) from the UVC lamp is reduced to 1/32 ($= 1/2^5$) of the UVC irradiation at the lamp surface. Therefore, it is considered that high concentration oxalic acid is mainly decomposed near the surface of UVC lamp, so strong turbulent mixing is required.

During the oxalate decomposition, vigorous bubbling was observed, as depicted in Fig. 3. This phenomenon is attributed to the uniform UVC irradiation to oxalic acid medium by turbulent mixing. Therefore, oxalate decomposition is supposed to proceed mainly via OH radical decomposition:

$$H_2C_2O_4 + 2\cdot OH \rightarrow 2CO_2 + 2H_2O \tag{10}$$

We experimentally confirmed that the decomposition product, CO_2, plays an important role of inducing turbulent mixing inside the reactor.

For comparison with the previous result [9], we compared the photo-Fenton AOP behavior observed when using UVA and UVC with similar oxalate concentrations (30 mmol/L). UVC radiation had much higher oxalate oxidation power than did UVA radiation, as shown in Fig. 4.

For a preliminary estimation of the parameters associated with the UVC photo-Fenton AOP for oxalate waste decomposition, the effect of the presence of each parameter was compared. The conditions for each experiment are shown in Table 1, and the decomposition percentage of the initial oxalate concentration (30 mmol/L) for an hour is shown in Fig. 5. In case of Exp. A, where all the three variables (UVC, H_2O_2 and Fenton reagent), 100% decomposition occurred. In Exp. B, where only UVC and H_2O_2 were used, about 50% decomposition was seen. The other cases showed less than 10% decomposition; in particular, almost no decomposition was seen in Exp. C, where UVC was not employed. These observations confirmed that both UVC irradiation and H_2O_2 play an important role in the decomposition of oxalic acid.

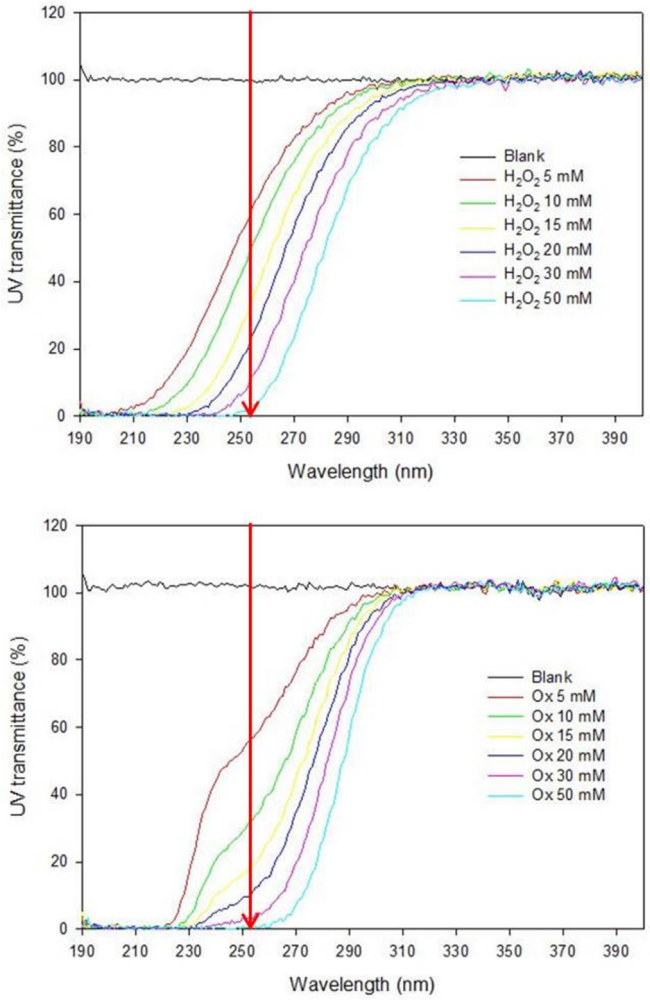

Fig. 2. UV transmittance (λ) depending on the H_2O_2 and oxalate concentrations.

3.2. Effect of H_2O_2 concentration depending on the oxalic acid concentration

During the application of the photo-Fenton treatment, it is important to find the optimal H_2O_2 dosage depending on the organic waste concentration [18]. Therefore, we attempted to select the proper range of H_2O_2 doses in the UVC/H_2O_2/Fe^{2+} treatment for the decomposition of high concentrations of oxalic acid. The volume of the oxalic waste and circulation flow rate were set at 3 L and 200 mL/min, respectively. The ferrous ion concentration was fixed as 2 mmol/L, which is reasonable concentration, considering the ferrous oxalate precipitation at a higher ferrous concentration. Thus, a large amount of Fe ions are included in the oxalate waste from the chemical decontamination of an NPP. Figs. 6–8 show the decomposition behavior for four different H_2O_2 initial concentrations, depending on the initial $H_2C_2O_4$ concentration. Experimental results showed that most of the oxalic acid was decomposed by UVC/H_2O_2/Fe^{2+} treatment within 90 min when the amount of H_2O_2 was equal to or greater than the oxalate concentration. Excess concentrations of H_2O_2, however, did not lead to any significant increase in the decomposition rate, implying that the surplus H_2O_2 would be self-decomposed, as indicated in equations (7) and (8). When the H_2O_2 concentration was lower than the oxalate concentration, a remarkable decrease in the decomposition rate was observed in all the experiments because of the H_2O_2 deficiency, and

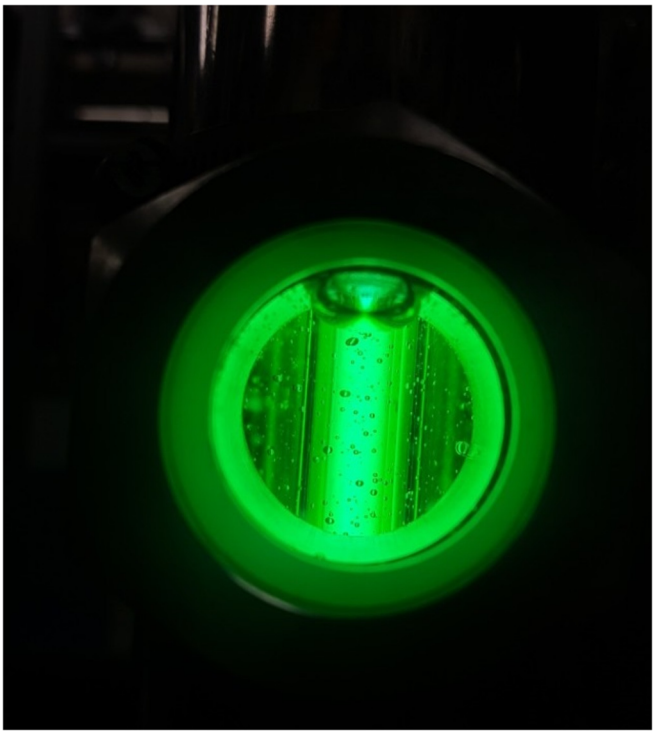

Fig. 3. Image of the vigorous mixing by CO_2 bubbling inside the UVC reactor.

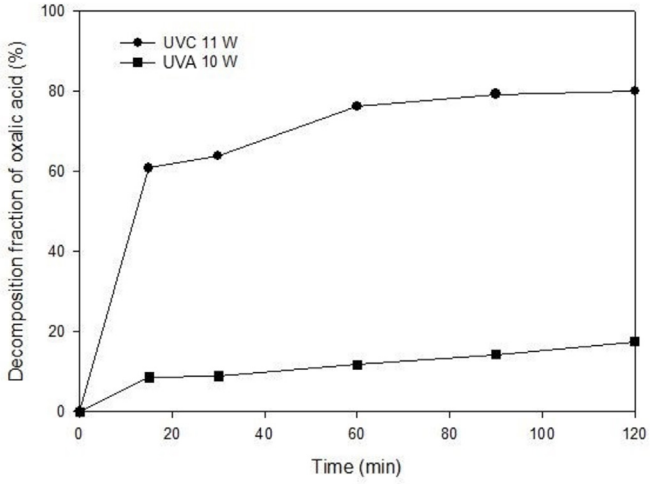

Fig. 4. Comparison of the oxalate decomposition behavior by UVA and UVC AOPs (initial concentrations of oxalic acid, H_2O_2, and ferrous ions: 30, 15, and 2 mmol/L, respectively).

Table 1
Conditions used in each experiment for comparing the effect of photo-Fenton parameters.

Experiment	Conditions		
	Fe^{2+} [mmol/L]	H_2O_2 [mmol/L]	UVC operation
Exp. A	2	30	ON
Exp. B	**0**	30	ON
Exp. C	2	30	**OFF**
Exp. D	2	**0**	ON

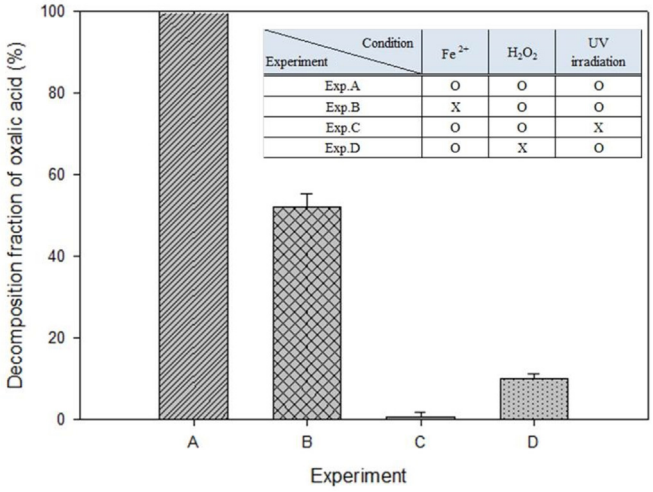

Fig. 5. Comparison of the decomposition fraction of oxalic acid depending on the process parameters.

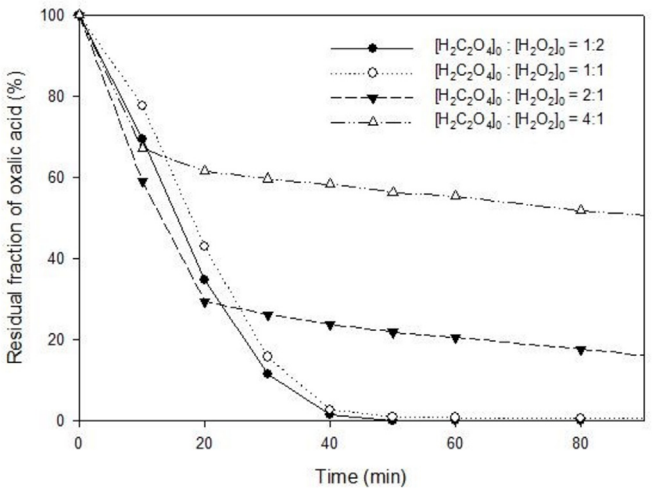

Fig. 6. Decomposition behavior of oxalic acid depending on the concentration ratio of hydrogen peroxide to oxalic acid (initial concentration of oxalic acid: 30 mmol/L).

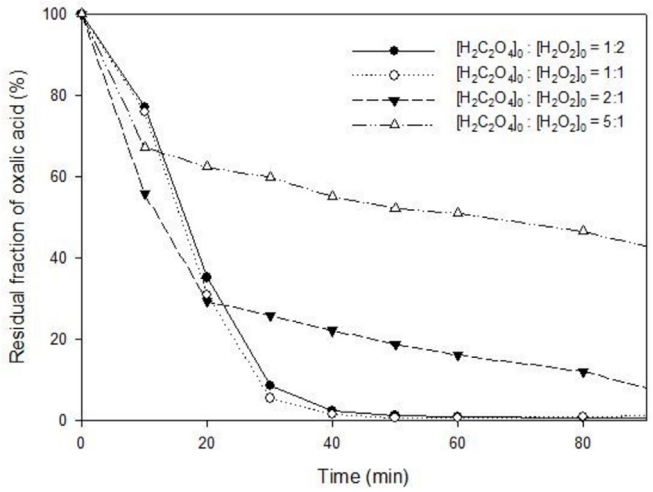

Fig. 7. Decomposition behavior of oxalic acid depending on the concentration ratio of hydrogen peroxide to oxalic acid (initial concentration of oxalic acid: 15 mmol/L).

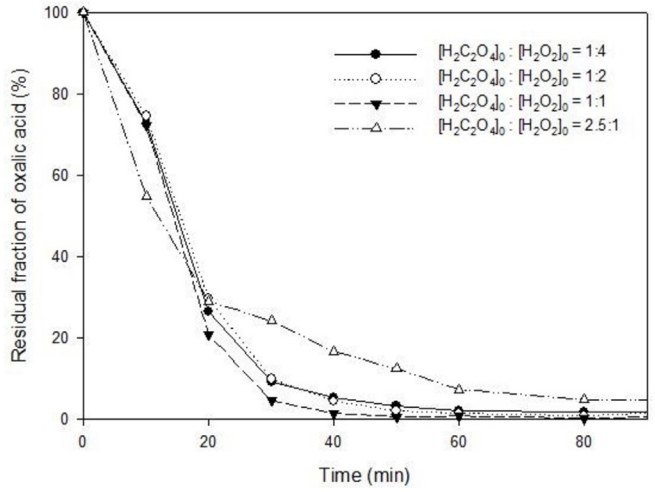

Fig. 8. Decomposition behavior of oxalic acid depending on the concentration ratio of hydrogen peroxide to oxalic acid (initial concentration of oxalic acid: 7.5 mmol/L).

the decomposition almost ceased when H_2O_2 was completely consumed. Therefore, the optimal amount of H_2O_2 was considered to be the same as the initial oxalate concentration.

The above results confirmed that the oxalate radical decomposition reaction followed equation (10) and that the OH radicals were mainly generated by UVC irradiation of H_2O_2, as shown in equation (4).

3.3. Decomposition behavior depending on the initial oxalate concentration

H_2O_2 was injected at a concentration equal to that of oxalic acid, and the decomposition behavior was compared for different initial oxalic acid concentrations (30, 15, and 7.5 mmol/L). In order to confirm the decomposition behavior at each initial concentration of oxalic acid, the residual fraction of oxalic acid was fitted with a first-order reaction model. The residual fraction of oxalic acid can be described by

$$X = \frac{C}{C_0} \times 100\ [\%] \tag{11}$$

where X is the residual fraction of oxalic acid in the photo-Fenton process; C and C_0 are the residual and initial concentrations of oxalic acid, respectively. The residual fraction X depending on the decomposition time can be expressed as a first-order reaction model, as shown in the following equations:

$$\frac{dX}{dt} = -kX \tag{12}$$

$$IC\ ; X(0) = X_0 = 100\ [\%] \tag{13}$$

$$X(t) = X_0 e^{-kt} = 100 e^{-kt} \tag{14}$$

where X_0 and k are the initial residual oxalic acid fraction and reaction rate constant, respectively. In this study, k, which is the parameter in equation (14), was derived from the experimental results by using the least-squares estimation, and the validity of the parameter value was judged by confirming whether R^2 was 0.9 or more.

Fig. 9 shows the selected decomposition behavior of oxalic acid for the same amount of H_2O_2 and oxalate depending on the initial concentration of oxalic acid from Figs. 6–8. The UVC photo-Fenton decomposition behavior predicted by the above reaction model fitted the experimental results well, with $R^2 \geq 0.93$, regardless of the initial concentration of oxalic acid.

3.4. Effect of UVC irradiation density on the decomposition behavior

3.4.1. Decomposition behavior in the once-through flow system

The decomposition behavior of oxalic acid as a function of the UVC irradiation time in the once-through reactor was investigated by varying the reactor residence time. The residence time corresponds to the UVC irradiation time of the oxalic acid waste, depending on the reactor flow rate. The UVC irradiation time for the once-through flow reactor, t, can be calculated as follows:

$$t = V_W / Q \tag{15}$$

where Vw [L] and Q [mL/min] are the volume of the reactor filled with oxalic acid and the flow rate in the once-through flow reactor, respectively.

The reactor volume was 3 L, and the flow rates were 50, 100, 200, 600, and 1200 mL/min. The decomposition fraction after one passage of the flow through the reactor was investigated by using two initial concentrations of 30 mmol/L and 15 mmol/L. Fig. 10 shows that the decomposition behavior followed the first-order reaction model in equation (14). There were no differences between the decomposition results obtained at the two initial concentrations of oxalic acid within the experimental error range.

The rate constant k for a waste volume (V_W) of 3 L and R^2 were 0.074 min^{-1} and 0.958, respectively. The first-order reaction rate constant can be expressed by a half-decay constant, t_h, as per the following relation:

$$t_h = \frac{ln2}{k} = 9.37\ \text{min} \tag{16}$$

3.4.2. Decomposition behavior in the circulation flow system

Experiments to monitor the decomposition behavior were carried out in a continuous circulation flow system, as shown in Fig. 1. The circulation flow rate of the waste was 200, 600, and 1200 mL/min; the waste volume was 6 L, where V_R is 3 L and V_T is 3 L.

Fig. 11 shows that the decomposition behavior followed the first-order reaction model in equation (14), and there were no significant differences with variations in the circulation rate in the reactor. From the experimental results and Fig. 3, which illustrates CO_2 bubbling in the reactor, the turbulent mixing induced by bubbling of CO_2 (product of oxalic acid decomposition in the UVC reactor) was thought to be sufficient to overcome the short penetration depth of the UVC energy in the concentrated oxalic acid and H_2O_2 medium in Fig. 2.

The reaction rate constant k for V_W of 6 L was 0.0375 min^{-1}, and the half-decay rate constant t_h was 18.5 min.

$$t_h = \frac{ln2}{k} = 18.5\ \text{min} \tag{17}$$

3.4.3. Dependence of decomposition behavior on UVC irradiation energy density

Comparison of the results for the two reactor flow systems, where V_W was 3 L and 6 L, respectively, revealed that the half-decay rate constant was approximately proportional to the waste volume

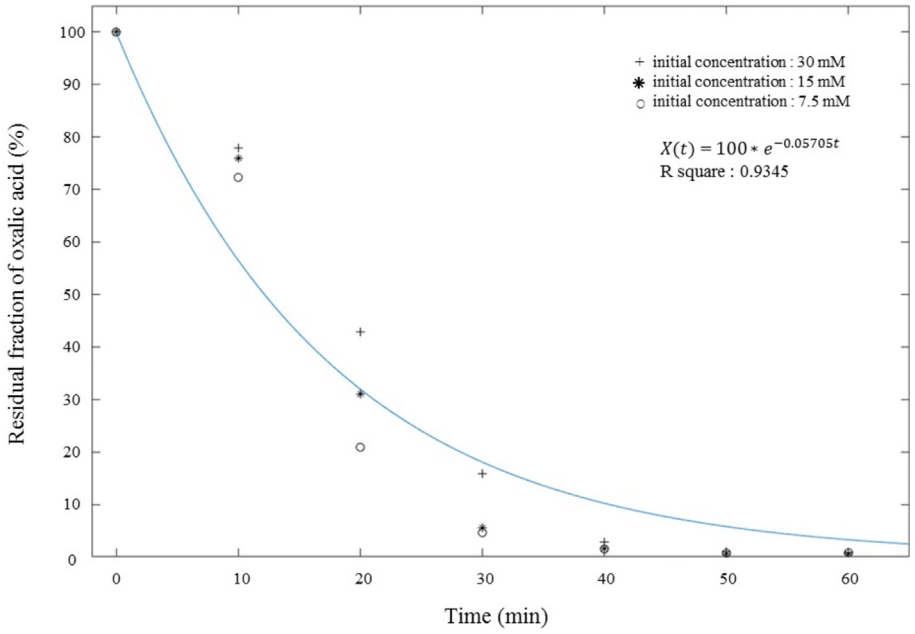

Fig. 9. Prediction of oxalic acid decomposition behavior with V_W of 3 L depending on oxalic acid concentration by a first-order reaction model (initial concentration ratio of oxalic acid to hydrogen peroxide = 1:1).

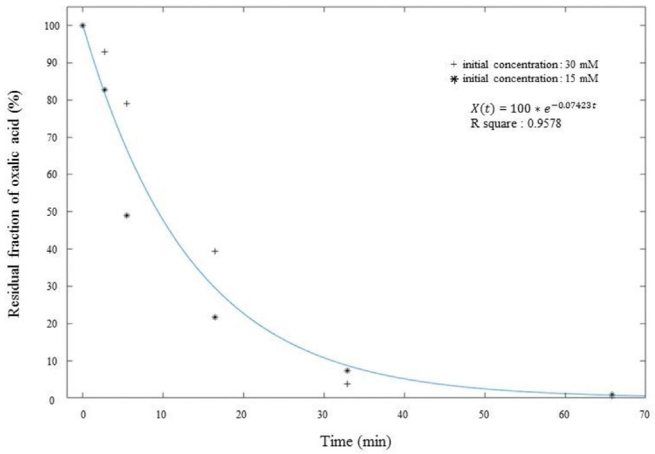

Fig. 10. Prediction by a first-order reaction model for oxalic acid decomposition behavior in the once-through flow system. Time = V_W/Q, where V_W = 3 L and Q = 50, 100, 200, 600, and 1200 mL/min.

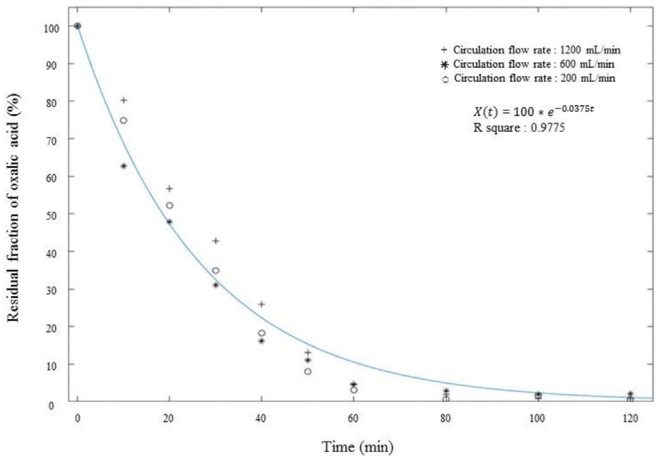

Fig. 11. Prediction of oxalic acid decomposition behavior in the circulation flow system with V_W of 6 L by a first-order reaction model.

subject to decomposition by UVC irradiation, which determines the reactor residence time of the waste flow:

$$\frac{18.5\,[mim]}{9.37[min]} = 1.97 \;\; and \;\; \frac{6[L]}{3[L]} = 2 \tag{18}$$

The results described in Sections 3.1–3.4.2, including the radical formation and termination reactions, indicate that the important variable influencing the UVC photo-Fenton decomposition is the UVC irradiation dose applied to the oxalic acid waste. We propose that the oxalate decomposition behavior can be expressed by a first-order kinetic model with respect to the UVC irradiation energy density (kJ/L) when the initial concentrations of oxalic acid and H_2O_2 are the same. Modification of equation (14) gives the following first-order reaction equations in terms of the UVC irradiation density for oxalate:

$$\rho_{UVC} = \frac{P_{UVC} \times t}{V_W} \tag{19}$$

$$\mathrm{kt} = \mathrm{k}\frac{V_W}{P_{UVC}} \times \rho_{UVC} = k_{UVC} \times \rho_{UVC} \tag{20}$$

$$\mathrm{X[\%]} = 100e^{-k_{UVC} \times \rho_{UVC}} \tag{21}$$

where t [min], ρ_{UVC} [kJ/L], P_{UVC} [kW], and V_W ($=V_R + V_T$) [L] are the reaction time, UVC energy density, UVC lamp power, and total waste volume, respectively.

In order to verify the above hypothesis, we recalculated the previous experimental results in Figs. 10 and 11, by using the UVC irradiation energy density. The data are collated in Table 2.

Table 2
Experimental conditions for determination of oxalic acid decomposition behavior depending on UVC energy irradiation methods and flow system.

Experiment (flow conditions)	$H_2C_2O_4$ [mmol/L]	$H_2C_2O_4$ waste volume, [L]			Circulation flow rate, Q [mL/min]	UVC [kW]
		V_R	V_T	V_W		
Once-through flow system	15 (*)	3	0	3	Q = 50, 100, 200, 600, 1200 and t = V_W/Q min	0.12
	30 (+)	3	0	3		
Circulation flow system	30	3	3	6	200 (◁)	
					600 (▷)	
					1200 (○)	

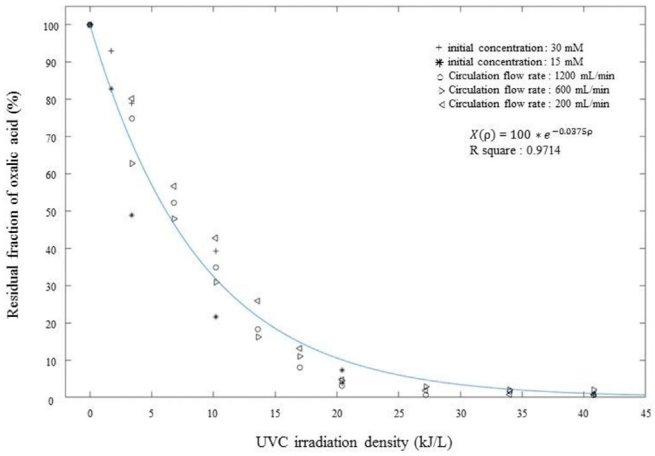

Fig. 12. Prediction of decomposition behavior using UVC irradiation energy density based on experimental results obtained with once-through and circulation flow systems.

Fig. 12 shows that the proposed UVC photo-Fenton decomposition model satisfactorily predicts the experimental results within the error range, with $R^2 = 0.97$.

4. Conclusions

The UVC photo-Fenton decomposition of oxalic acid waste obtained from the chemical decontamination of an NPP was investigated. By carrying out experiments on the effects of UVC energy, H_2O_2 concentration, circulation rate, oxalic acid concentration, and waste volume, the following conclusions were obtained within the experimental range.

1. The rate-determining radical reactions are ·OH formation by UVC irradiation of H_2O_2 and oxalic acid decomposition by ·OH radicals to produce CO_2 and H_2O, as follows:

$$H_2O_2 + hv \rightarrow 2\ \cdot OH$$

$$H_2C_2O_4 + 2\cdot OH \rightarrow 2CO_2 + 2H_2O$$

2. The oxalic acid decomposition rate can be expressed as a first-order reaction based on the oxalic acid concentration, and the UVC photo-Fenton decomposition behavior of oxalic acid can be expressed in terms of the UVC energy irradiation density, regardless of the circulation rate and reactor volume:

$$X = 100e^{-0.0375\times\rho_{UVC}}\ [\%]$$

where $\rho_{UVC} = \frac{P_{UVC}\times t}{V_W}$ [kJ/L]; t [min], ρ_{UVC} [kJ/L], P_{UVC} [kW], and V_W [L] are the reaction time, UVC energy density, UVC lamp power, and total waste volume, respectively.

3. The optimal initial H_2O_2 concentration is about the same as the initial oxalic acid concentration in the UVC photo-Fenton decomposition of oxalate waste.

Acknowledgement

This work was supported by the Korea Institute of Energy Technology Evaluation and Planning and the Ministry of Trade, Industry and Energy of the Republic of Korea (No. 2014151030031).

References

[1] F.J. Beltrán, F.J. Rivas, R. Montero-de-Espinosa, Iron type catalysts for the ozonation of oxalic acid in water, Water Res. 39 (15) (2005) 3553–3564.
[2] M. Dükkancı, G. Gündüz, Ultrasonic degradation of oxalic acid in aqueous solutions, Ultrason. Sonochem. 13 (6) (2006) 517–522.
[3] Y.H. Huang, Y.J. Shih, C.H. Liu, Oxalic acid mineralization by electrochemical oxidation processes, J. Hazard Mater. 188 (1–3) (2011) 188–192.
[4] M.M. Kosanić, Photocatalytic degradation of oxalic acid over TiO_2 power, J. Photochem. Photobiol. A Chem. 119 (2) (1998) 119–122.
[5] T. Zhang, Modeling Photolytic Advanced Oxidation Processes for the Removal of Trace Organic Contaminants, PhD Thesis, department of chemical and environmental engineering, Arizona University, 2017, pp. 2–33.
[6] C. Lee, J. Yoon, Determination of quantum yields for the photolysis of Fe (III)-hydroxo complexes in aqueous solution using a novel kinetic method, Chemosphere 57 (10) (2004) 1449–1458.
[7] J.A. Zazo, et al., Chemical pathway and kinetics of phenol oxidation by Fenton's reagent, Environ. Sci. Technol. 39 (23) (2005) 9295–9302.
[8] L.A. Pérez-Estrada, et al., Photo-Fenton degradation of diclofenac: identification of main intermediates and degradation pathway, Environ. Sci. Technol. 39 (21) (2005) 8300–8306.
[9] Q. Natalia, et al., Oxalic acid destruction at high concentrations by combined heterogeneous photocatalysis and photo-Fenton processes, Catal. Today 101 (2005) 253–260.
[10] M. Nagase, et al., Low corrosive chemical decontamination method using pH control, (I) basic system, J. Nucl. Sci. Technol. 38 (12) (2001) 1090–1096.
[11] D.I. Metelitsa, Mechanisms of the hydroxylation of aromatic compounds, Russ. Chem. Rev. 40 (7) (1971) 563–580.
[12] F. Haber, J. Weiss, The catalytic decomposition of hydrogen peroxide by iron salts, Proc. Roy. Soc. Lond. A 147 (861) (1934) 332–351.
[13] E. Brillas, I. Sirés, M.A. Oturan, Electro-Fenton process and related electrochemical technologies based on Fenton's reaction chemistry, Chem. Rev. 109 (12) (2009) 6570–6631.
[14] P. Vrushali, G. Sagar, An overview of the Fenton process for industrial waste water, J. Mech. Civil Eng. (2016) 127–136.
[15] M.A. Oturan, J.J. Aaron, Advanced oxidation processes in water/wastewater treatment: principles and applications, A review, Critical Reviews Environ. Sci. Technol. 44 (23) (2014) 2577–2641.
[16] Machulek Jr., et al., Fundamental Mechanistic Studies of the Photo-Fenton Reaction for the Degradation of Organic Pollutants, Organic Pollutants Ten Years after the Stockholm Convention-Environmental and Analytical Update, 2012.
[17] S.O. Lee, T. Tran, B.H. Jung, S.J. Kim, M.J. Kim, Dissolution of iron oxide using oxalic acid, Hydrometallurgy 87 (3–4) (2007) 91–99.
[18] N.H. Ince, D.T. Gönenç, Treatability of a textile azo dye by UV/H_2O_2, Environ. Technol. 18 (2) (1997) 179–185.